Inhomogeneous broadening of tunneling conductance in double quantum wells

F. T. Vasko
Institute of Semiconductor Physics, National Academy of Sciences, 45 Prospekt Nauky, Kiev, 252650, Ukraine

O. G. Balev* and Nelson Studart
Departmento de Física, Universidade Federal de São Carlos, 13565-905, São Carlos, São Paulo, Brazil
(Received 19 June 2000)

The line shape of the tunneling conductance in double quantum wells with a large-scale roughness of heterointerfaces is investigated. Large-scale variations of coupled energy levels and scattering due to the short-range potential are taken into account. The interplay between the inhomogeneous broadening, induced by the nonscreened part of large-scale potential, and the homogeneous broadening due to scattering by short-range potentials is considered. It is shown that the large inhomogeneous broadening can be strongly modified by nonlocal effects involved in the proposed mechanism of inhomogeneity. The related change of the line shape of the resonant tunneling conductance between Gaussian and Lorentzian peaks is described. The theoretical results agree quite well with experimental data.

I. INTRODUCTION

Resonant tunneling in semiconductor heterostructures has been widely investigated ever since Tsu and Esaki proposed the double-barrier resonant-tunneling diode[1] (see Ref. 2 for a recent review). New developments came through from studies of interlayer tunneling spectroscopy between parallel two-dimensional (2D) electron systems (2DES) using the technique of independent contacts to closely located 2DES.[3,4] The 2DES are formed in two GaAs quantum wells (QW's) separated by an $Al_xGa_{1-x}As$ barrier. Because the in-plane momentum and the energy are conserved, the 2D-2D tunneling current exhibits sharp resonance peak whose broadening is determined by different collision processes in the nonideal double-quantum-well (DQW) structure. This property allows us to study scattering mechanisms through tunneling spectroscopy method.[5] Furthermore, broadening effects may be important in a novel quantum transistor based on 2D-2D tunneling in independently contacted DQW's.[6]

The aim of this paper is to describe the line shape of the resonant tunneling current in nonideal DQW's with independent contacts to each QW, when, in addition to usual homogeneous broadening induced by short-range scattering, the inhomogeneous broadening due to large-scale variations of heterointerfaces is taken into account. The latter mechanism has an essential effect on the form of the peak, because smooth variations of the DQW energy levels due to large-scale random variations of the widths of right and left QW's cannot be screened, even though the screening potential involves all possible redistributions of electrons within the DQW structure. Even though the averaged large-scale potential is screened in heavily doped structures, the intersubband energy is still nonuniform over the plane of the quantum well. In Fig. 1, a schematic view of the band diagram of DQW's and spatial variations of the energy levels are depicted for illustration. Our theory is valid when the DQW width is smaller than the correlation length l_c for nonuniformities of the heterointerfaces in the DQW. A very similar mechanism was recently proposed in a single quantum well for describing the inhomogeneous broadening of intersubband transitions, with one subband occupancy,[7] and for new effects in classical magnetotransport in the case of double subband occupancy.[8] The possibility of inhomogeneous broadening of the tunneling conductance peak due to large-scale impurity potential was briefly introduced in Ref. 9. However, in this work the construction of the nonscreened potential in DQWs is not discussed and comparison with experiment is absent.

We show that the Lorentzian line shape for the tunneling current peak, in the case of short-range collision-induced broadening, assumes a Gaussian shape due to inhomogeneous broadening if nonlocal effects are discarded due to sufficiently large l_c. However, for not too large l_c, we obtain the transformation from a Gaussian to Lorentzian line shape due to nonlocal effects on the inhomogeneous broadening. Moreover, inhomogeneous and nonlocal effects essentially modify the half width at half maximum (HWHM) of the peak. As is shown below, our theoretical results are in quite reasonable agreement with the experimental ones of Ref. 5.

The paper is organized in the following way. In Sec. II we evaluate the expression for the tunneling current up to second order in the weak interwell tunneling coupling and use the path-integral representation to calculate the tunneling conductance in terms of the averaged product of Green's functions for electron in left and right QW's. The line shape of the resonant tunneling conductance is analyzed in Sec. III

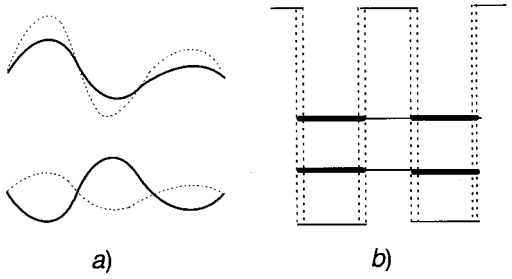

FIG. 1. (a) Spatial variations of the energy levels in left and right QW's along the x direction without screening (dotted curves) and with screening (solid curves); (b) band diagram of DQW's, along the z direction, with nonideal heterointerfaces shown by dashed lines.

in a quasiclassical approximation. The list of assumptions and concluding remarks are given in Sec. IV. Appendix A contains estimates of the parameters used in the nonscreened potential, due to large-scale nonuniformities of the heterointerfaces, and in Appendix B we briefly discuss the optimal fluctuation method and the straightforward trajectory approximation used in Sec. III.

II. TUNNELING CURRENT

Electron states in left (l) and right (r) QW's are described by the Hamiltonians

$$\hat{H}_l=\Delta+\frac{\hat{p}^2}{2m}+\overline{U}_{l\mathbf{x}}+\tilde{U}_{l\mathbf{x}}+V_{\mathbf{x}},$$
$$\hat{H}_r=\frac{\hat{p}^2}{2m}+\overline{U}_{r\mathbf{x}}+\tilde{U}_{r\mathbf{x}}+V_{\mathbf{x}}, \tag{1}$$

where Δ is the interlevel splitting without tunneling and m is the effective mass. The effect of fluctuations of heterointerfaces and scattering processes are described by large-scale and short-range potentials $\overline{U}_{l,r\mathbf{x}}$ and $\tilde{U}_{l,r\mathbf{x}}$ in left and right QW's. The screening potential, $V_{\mathbf{x}}$, included in $\hat{H}_{l,r}$, is determined from the Poisson equation (see Appendix A) and only the averaged large-scale potential is screened as

$$\frac{\overline{U}_{l\mathbf{x}}+\overline{U}_{r\mathbf{x}}}{2}+V_{\mathbf{x}}=0. \tag{2}$$

Taking into account the interwell tunneling coupling, we use a 2×2 one-electron Hamiltonian matrix as

$$\begin{vmatrix}\hat{h}_l & T\\ T & \hat{h}_r\end{vmatrix}, \tag{3}$$

where the diagonal terms are given by

$$\hat{h}_l=\Delta+\frac{\hat{p}^2}{2m}+\tilde{U}_{l\mathbf{x}}+\frac{\delta U_{\mathbf{x}}}{2},$$
$$\hat{h}_r=\frac{\hat{p}^2}{2m}+\tilde{U}_{r\mathbf{x}}-\frac{\delta U_{\mathbf{x}}}{2},$$

the nonscreening part of the large-scale potential is $\delta U_{\mathbf{x}}=\overline{U}_{l\mathbf{x}}-\overline{U}_{r\mathbf{x}}$, and the nondiagonal terms are given by the tunneling matrix element T (the coupling energy). In the following, we assume that the random potentials introduced above are statistically independent and described by Gaussian correlation functions

$$\langle\tilde{U}_{j\mathbf{x}}\tilde{U}_{j'\mathbf{x}}\rangle=\delta_{jj'}\tilde{W}_j(|\mathbf{x}-\mathbf{x}'|),\quad \langle\overline{U}_{j\mathbf{x}}\overline{U}_{j'\mathbf{x}}\rangle=\delta_{jj'}\overline{W}_j(|\mathbf{x}-\mathbf{x}'|),$$
$$\langle\delta U_{\mathbf{x}}\delta U_{\mathbf{x}'}\rangle=\overline{W}_l(|\mathbf{x}-\mathbf{x}'|)+\overline{W}_r(|\mathbf{x}-\mathbf{x}'|)\equiv w(|\mathbf{x}-\mathbf{x}'|), \tag{4}$$

where the functions $\overline{W}_{l,r}(\mathbf{x})$ and $w(\mathbf{x})$ are discussed in Appendix A. We also neglect here the in-plane variations of the matrix element T (see discussion in Ref. 10).

The interwell tunneling current is expressed in terms of the density matrix $\hat{\rho}_t$ according to[10,11]

$$J_\perp=\frac{|e|T}{\hbar}\frac{2}{L^2}\mathrm{tr}(\hat{\sigma}_y\hat{\rho}_t),\quad \hat{\rho}_t=\begin{vmatrix}\hat{\rho}_{lt} & \tilde{\rho}_t\\ \tilde{\rho}_t^+ & \hat{\rho}_{rt}\end{vmatrix}, \tag{5}$$

where $\hat{\sigma}_y$ is the y component of the Pauli matrix and the trace includes both the average over large-scale and short-range random potentials and the summation over electron states. Nondiagonal and diagonal components of the density matrix in Eq. (5) are connected by the relation ($\delta\to+0$)

$$\tilde{\rho}_t=\frac{iT}{\hbar}\int_{-\infty}^{t}dt'e^{\delta t'}e^{-i\hat{h}_l(t-t')/\hbar}(\hat{\rho}_{lt'}-\hat{\rho}_{rt'})e^{i\hat{h}_r(t-t')/\hbar}. \tag{6}$$

Using a set of wave functions $(\mathbf{x}|j\lambda)\equiv\psi_{j\mathbf{x}}^{\lambda}$ that are determined by the eigenvalue problems in the jth QW $\hat{h}_j\psi_{j\mathbf{x}}^{\lambda}=\varepsilon_{j\lambda}\psi_{j\mathbf{x}}^{\lambda}$ we rewrite the tunneling current (5) as

$$J_\perp=i\frac{|e|T}{\hbar}\frac{2}{L^2}\left\langle\left\langle\sum_{\lambda}\left[(r\lambda|\tilde{\rho}_t|r\lambda)-(l\lambda|\tilde{\rho}_t^+|l\lambda)\right]\right\rangle\right\rangle. \tag{7}$$

Here $\langle\langle\cdots\rangle\rangle$ means the average over short-range and large-scale potentials. After substitution of Eq. (6) in Eq. (7), we obtain

$$J_\perp=\frac{2\pi|e|T^2}{\hbar}\frac{2}{L^2}\left\langle\left\langle\sum_{\lambda\lambda'}|(r\lambda|l\lambda')|^2\delta(\varepsilon_{r\lambda}-\varepsilon_{l\lambda'})(f_{r\lambda}-f_{l\lambda'})\right\rangle\right\rangle$$
$$=\frac{2\pi|e|T^2}{\hbar}\frac{2}{L^2}\int_{\varepsilon_{Fl}}^{\varepsilon_{Fr}}d\varepsilon\left\langle\left\langle\sum_{\lambda\lambda'}|(r\lambda|l\lambda')|^2\delta(\varepsilon_{r\lambda}-\varepsilon)\delta(\varepsilon-\varepsilon_{l\lambda'})\right\rangle\right\rangle, \tag{8}$$

where the second equation above is written for the zero-temperature case and ε_{Fj} is the quasi-Fermi-level in the jth QW.

In order to calculate $J_\perp$, it is convenient to use the retarded (R) Green's functions for the electron in left and right QW's, which are defined as

$$\mathcal{G}_{j\varepsilon}^{R}(\mathbf{x},\mathbf{x}')=\sum_{\lambda}\frac{\psi_{j\mathbf{x}'}^{\lambda *}\psi_{j\mathbf{x}}^{\lambda}}{(\varepsilon_{j\lambda}-\varepsilon-i\delta)}, \tag{9}$$

and the advanced (A) Green's functions given by $\mathcal{G}_{j\varepsilon}^{A}(\mathbf{x},\mathbf{x}')$

$=\mathcal{G}^R_{j\varepsilon}(\mathbf{x}',\mathbf{x})^*$. The tunneling current assumes the form

$$J_\perp=\frac{|e|T^2}{2\pi\hbar}\frac{2}{L^2}\int_{\varepsilon_{Fl}}^{\varepsilon_{Fr}}d\varepsilon\int d\mathbf{x}\int d\mathbf{x}' \times\sum_{ab=RA}(-1)^k\langle\langle\mathcal{G}^a_{l\varepsilon}(\mathbf{x},\mathbf{x}')\mathcal{G}^b_{r\varepsilon}(\mathbf{x}',\mathbf{x})\rangle\rangle, \quad (10)$$

where $k=1$ for $a=b$ and $k=0$ for $a\neq b$. For small applied voltages satisfying $|\varepsilon_{Fl}-\varepsilon_{Fr}|\ll\varepsilon_{Fr,l}\simeq\varepsilon_F$, we introduce the tunneling conductance, $\mathfrak{G}(\Delta)$, through the relation $J_\perp=\mathfrak{G}(\Delta)V$. The interwell voltage V is connected with the quasi-Fermi-level difference by the relation $V=(\varepsilon_{Fl}-\varepsilon_{Fr})/e$. Then from Eq. (10) it follows that the tunneling conductance can be written as

$$\mathfrak{G}(\Delta)=\frac{(eT)^2}{2\pi\hbar}\frac{2}{L^2}\int d\mathbf{x}\int d\mathbf{x}' \times\sum_{ab=RA}(-1)^k\langle\langle\mathcal{G}^a_{l\varepsilon_F}(\mathbf{x},\mathbf{x}')\mathcal{G}^b_{r\varepsilon_F}(\mathbf{x}',\mathbf{x})\rangle\rangle. \quad (11)$$

Furthermore, according to Eq. (4), the short-range potentials in the left and right QW's are statistically independent, then the two-particle correlation function $\langle\langle\cdots\rangle\rangle$ in Eq. (11) can be rewritten exactly in terms of the Green's functions $G^a_{j\varepsilon}(\mathbf{x},\mathbf{x}')=\langle\mathcal{G}^a_{j\varepsilon}(\mathbf{x},\mathbf{x}')\rangle$ averaged over the short-range potentials. The Dyson equation for this Green's functions is written as

$$(\tilde{h}_j-\varepsilon)G^a_{j\varepsilon}(\mathbf{x},\mathbf{x}')+\int d\mathbf{x}_1\Sigma^a_{j\varepsilon}(\mathbf{x},\mathbf{x}_1)G^a_{j\varepsilon}(\mathbf{x}_1,\mathbf{x}')=\delta(\mathbf{x}-\mathbf{x}'). \quad (12)$$

Here the Hamiltonians $\tilde{h}_{l,r}$ coincide with those given in Eq. (3), without the short-range potentials $\tilde{U}_{l,r\mathbf{x}}$, and $\Sigma^a_{j\varepsilon}(\mathbf{x},\mathbf{x}')$ is the self-energy function. For δ-correlated potentials, we have to use $\Sigma^a_{j\varepsilon}(\mathbf{x},\mathbf{x}')\propto\delta(\mathbf{x}-\mathbf{x}')$. Neglecting the renormalization of energy spectra, we rewrite Eq. (12) in terms of the broadening energy γ_j of the jth QW as

$$(\tilde{h}_j-\varepsilon\mp i\gamma_j)G^{R,A}_{j\varepsilon}(\mathbf{x},\mathbf{x}')=\delta(\mathbf{x}-\mathbf{x}'), \quad (13)$$

where the upper sign corresponds to G^R and the lower one to G^A.

It is convenient to write the Green's functions through path integrals as[12,13]

$$G^R_{l\varepsilon}(\mathbf{x},\mathbf{x}')=\frac{i}{\hbar}\int_{-\infty}^0 dt\,e^{-i(\varepsilon+i\gamma_l-\Delta)t/\hbar}\int_{\mathbf{x}_0=\mathbf{x}'}^{\mathbf{x}_t=\mathbf{x}}\mathcal{D}\{\mathbf{x}_\tau\} \times\exp\left[-\frac{i}{2\hbar}\int_0^t d\tau(m\dot{\mathbf{x}}_\tau^2-\delta U_{\mathbf{x}_\tau})\right],$$

$$G^R_{r\varepsilon}(\mathbf{x},\mathbf{x}')=\frac{i}{\hbar}\int_{-\infty}^0 dt\,e^{-i(\varepsilon+i\gamma_r)t/\hbar}\int_{\mathbf{x}_0=\mathbf{x}'}^{\mathbf{x}_t=\mathbf{x}}\mathcal{D}\{\mathbf{x}_\tau\} \times\exp\left[-\frac{i}{2\hbar}\int_0^t d\tau(m\dot{\mathbf{x}}_\tau^2+\delta U_{\mathbf{x}_\tau})\right], \quad (14)$$

and $G^A_{j\varepsilon}(\mathbf{x},\mathbf{x}')=G^R_{j\varepsilon}(\mathbf{x}',\mathbf{x})^*$. The average over the nonscreened large-scale potential in Eq. (11), for a Gaussian-type random potential $\delta U_{\mathbf{x}}$, is performed using the well-known exact formula

$$\left\langle\exp\left(\int d\mathbf{x}\,f_{\mathbf{x}}\delta U_{\mathbf{x}}\right)\right\rangle=\exp\left[\frac{1}{2}\int d\mathbf{x}\int d\mathbf{x}'f_{\mathbf{x}}w(|\mathbf{x}-\mathbf{x}'|)f_{\mathbf{x}'}\right], \quad (15)$$

for some arbitrary function $f_{\mathbf{x}}$. Since random potentials are involved in both path integrals, we choose these functions as

$$f_{\mathbf{x}}=\pm(i/2\hbar)\int_0^{t_1}d\tau_1\delta(\mathbf{x}-\mathbf{x}_{\tau_1})\pm(i/2\hbar)\int_0^{t_2}d\tau_2\delta(\mathbf{x}-\mathbf{x}_{\tau_2}).$$

Using these transformations in the correlation functions of Eq. (11), we finally obtain

$$\begin{aligned}\sum_{ab=RA}(-1)^k\langle G^a_{l\varepsilon_F}(\mathbf{x},\mathbf{x}')G^b_{r\varepsilon_F}(\mathbf{x}',\mathbf{x})\rangle &=\frac{1}{\hbar^2}\int_{-\infty}^0 dt_1e^{(\gamma_l+i\Delta)t_1/\hbar}\int_{-\infty}^0 dt_2e^{\gamma_rt_2/\hbar}\int_{\mathbf{x}_0=\mathbf{x}'}^{\mathbf{x}_{t_1}=\mathbf{x}}\mathcal{D}\{\mathbf{x}_\tau\}\\ &\times\left\{e^{-i\varepsilon_F(t_1+t_2)/\hbar}\int_{\mathbf{y}_0=\mathbf{x}}^{\mathbf{y}_{t_2}=\mathbf{x}'}\mathcal{D}\{\mathbf{y}_\tau\}\exp[-\mathcal{S}_+(t_1t_2|\mathbf{x}_\tau,\mathbf{y}_\tau)]\right.\\ &\left.+e^{-i\varepsilon_F(t_1-t_2)/\hbar}\int_{\mathbf{y}_0=\mathbf{x}'}^{\mathbf{y}_{t_2}=\mathbf{x}}\mathcal{D}\{\mathbf{y}_\tau\}\exp[-\mathcal{S}_-(t_1t_2|\mathbf{x}_\tau,\mathbf{y}_\tau)]\right\}\\ &+\text{c.c.}, \end{aligned} \quad (16)$$

where the two-particle actions $\mathcal{S}_\pm(t_1t_2|\mathbf{x}_\tau,\mathbf{y}_\tau)$ are written in the form

$$\begin{aligned}\mathcal{S}_\pm(t_1t_2|\mathbf{x}_\tau,\mathbf{y}_\tau)=\frac{im}{2\hbar}\left[\int_0^{t_1}d\tau\dot{\mathbf{x}}_\tau^2\pm\int_0^{t_2}d\tau\dot{\mathbf{y}}_\tau^2\right]&+\frac{1}{8\hbar^2}\int_0^{t_1}d\tau\int_0^{t_1}d\tau'w(|\mathbf{x}_\tau-\mathbf{x}_{\tau'}|)\\ &+\frac{1}{8\hbar^2}\int_0^{t_2}d\tau\int_0^{t_2}d\tau'w(|\mathbf{y}_\tau-\mathbf{y}_{\tau'}|)\\ &\mp\frac{1}{4\hbar^2}\int_0^{t_1}d\tau\int_0^{t_2}d\tau'w(|\mathbf{x}_\tau-\mathbf{y}_{\tau'}|). \end{aligned} \quad (17)$$

Substituting Eq. (16) into Eq. (11) and making convenient change of variables (in particular, separating the straight path according to $\mathbf{x}_\tau\to[\mathbf{u}\tau/t_1+\mathbf{x}_\tau]$ and $\mathbf{y}_\tau\to[\mathbf{u}(t_2-\tau)/t_2+\mathbf{y}_\tau]$, for integral from $\exp(-\mathcal{S}_+)$, or $\mathbf{y}_\tau\to[\mathbf{u}\tau/t_2+\mathbf{y}_\tau]$, for integral from $\exp(-\mathcal{S}_-)$), we can express $\mathfrak{G}(\Delta)$ in terms of contour integrals as

$$\mathcal{G}(\Delta)=\frac{(eT)^2}{\pi\hbar^3}\int d\mathbf{u}\int_{-\infty}^{0}dt_1 e^{(\gamma_l+i\Delta)t_1/\hbar}\times\int_{-\infty}^{0}dt_2 e^{\gamma_r t_2/\hbar}\oint\mathcal{D}\{\mathbf{x}_\tau\}\oint\mathcal{D}\{\mathbf{y}_\tau\}\sum_{\pm}\times\left\{e^{-i\varepsilon_F(t_1\pm t_2)/\hbar}\exp\left[-\frac{im}{2\hbar}\mathbf{u}^2(t_1^{-1}\pm t_2^{-1})\right]\times\exp\left[-\frac{im}{2\hbar}\left(\int_0^{t_1}d\tau\,\dot{\mathbf{x}}_\tau^2\pm\int_0^{t_2}d\tau\,\dot{\mathbf{y}}_\tau^2\right)\right]\times\exp[-K_\pm(t_1,t_2,\mathbf{x}_\tau,\mathbf{y}_\tau)]\right\}+\text{c.c.},\tag{18}$$

where $\mathbf{u}=\mathbf{x}-\mathbf{x}'$. The contributions of nonscreened potentials to the correlation function is given by the factors

$$K_\pm(t_1,t_2,\mathbf{x}_\tau,\mathbf{y}_\tau)=\frac{1}{8\hbar^2}\int_0^{t_1}d\tau\int_0^{t_1}d\tau' w(|\mathbf{x}_\tau-\mathbf{x}_{\tau'}+\mathbf{u}(\tau-\tau')/t_1|)+\frac{1}{8\hbar^2}\int_0^{t_2}d\tau\int_0^{t_2}d\tau' w(|\mathbf{y}_\tau-\mathbf{y}_{\tau'}\pm\mathbf{u}(\tau-\tau')/t_2|)\mp\frac{1}{4\hbar^2}\int_0^{t_1}d\tau\int_0^{t_2}d\tau' w_\pm(|\mathbf{x}_\tau-\mathbf{y}_{\tau'}+\mathbf{u}(\tau/t_1\pm\tau'/t_2)|)\tag{19}$$

with $w_-(|\mathbf{z}|)=w(|\mathbf{z}|)$ and $w_+(|\mathbf{z}|)=w(|\mathbf{z}-\mathbf{u}|)$. Note that K_+ comes from averaging both retarded or both advanced Green's functions while K_- corresponds to averaging the product of retarded and advanced Green's functions.

III. LINE SHAPE OF THE CONDUCTANCE PEAK

In order to calculate the path integrals in Eq. (18), we will neglect in Eqs. (18) and (19) deviations $\mathbf{x}_\tau$ and $\mathbf{y}_\tau$ in the arguments of the correlation function $w(|\cdots|)$ by supposing that these deviations are smaller than l_c, i.e., using the approach of straightforward trajectory in Eq. (19). We justify such an approximation in Appendix B, where the optimal fluctuation method[14] is used, in order to extract the optimal trajectories that give the maximal contribution to the path integrals. With this approximation, we can calculate the path integrals for the free motion exactly and the conductance, given by Eq. (18), is rewritten as

$$\mathcal{G}(\Delta)=\frac{(eT)^2}{\pi\hbar^3}\int d\mathbf{u}\int_{-\infty}^{0}dt_1 e^{(\gamma_l+i\Delta)t_1/\hbar}\times\int_{-\infty}^{0}dt_2 e^{\gamma_r t_2/\hbar}\frac{(m/2\pi\hbar)^2}{t_1t_2}\times\sum_{\pm}\left[\mp e^{-i\varepsilon_F(t_1\pm t_2)/\hbar}\exp\left(-\frac{imu^2}{2\hbar}(t_1^{-1}\pm t_2^{-1})-K_\pm(t_1,t_2,u)\right)\right]+\text{c.c.},\tag{20}$$

where the factors $K_\pm$ are reduced to

$$K_\pm(t_1,t_2,u)=\frac{1}{8\hbar^2}\int_0^{t_1}d\tau\int_0^{t_1}d\tau' w(u|\tau-\tau'|/t_1)+\frac{1}{8\hbar^2}\int_0^{t_2}d\tau\int_0^{t_2}d\tau' w(u|\tau-\tau'|/t_2)\mp\frac{1}{4\hbar^2}\int_0^{t_1}d\tau\int_0^{t_2}d\tau' w_\pm(|\mathbf{u}(\tau/t_1\pm\tau'/t_2)|).\tag{21}$$

Let us for a moment ignore the contribution from the terms with the upper sign in Eq. (20). Defining new variables $x=\tau/t_{1,2}$ and $x'=\tau'/t_{1,2}$ in the factor $K_-(t_1,t_2,u)$, we obtain the conductance in the form

$$\mathcal{G}(\Delta)=\frac{(eT)^2}{\pi\hbar^3}\int d\mathbf{u}\int_{-\infty}^{0}dt_1 e^{(\gamma_l+i\Delta)t_1/\hbar}\times\int_{-\infty}^{0}dt_2 e^{\gamma_r t_2/\hbar}\frac{(m/2\pi\hbar)^2}{t_1t_2}e^{-i\varepsilon_F(t_1-t_2)/\hbar}\times\exp\left[-\frac{imu^2}{2\hbar}(t_1^{-1}-t_2^{-1})-\frac{(t_1+t_2)^2}{8\hbar^2}W\left(\frac{u}{l_c}\right)\right]+\text{c.c.},\tag{22}$$

where the large-scale correlation function is transformed as $W(u/l_c)=\overline{\delta\varepsilon^2}\int_0^1dx\int_0^1dx'\exp[-(u/l_c)^2(x-x')^2]$ and can be rewritten as

$$W(x)/\overline{\delta\varepsilon^2}=\sqrt{\pi}x^{-1}\,\mathrm{erf}(x)-x^{-2}[1-e^{-x^2}],\tag{23}$$

and $\mathrm{erf}(x)$ is the error function. Introducing new time variables $\tau=t_1-t_2$ and $t=(t_1+t_2)/2$ it follows that

$$\mathcal{G}(\Delta)=\frac{(eT)^2}{\pi\hbar^3}\int d\mathbf{u}\int_{-\infty}^{0}dt\int_{2t}^{-2t}\times d\tau\, e^{(\gamma t+\Delta\gamma\tau)/\hbar}\frac{(m/2\pi\hbar)^2}{t^2-\tau^2/4}e^{i[\Delta(t+\tau/2)-\varepsilon_F\tau]/\hbar}\times\exp\left[\frac{imu^2}{2\hbar}\frac{\tau}{t^2-\tau^2/4}-\frac{t^2}{2\hbar^2}W\left(\frac{u}{l_c}\right)\right]+\text{c.c.},\tag{24}$$

where $\gamma=\gamma_l+\gamma_r$ and $\Delta\gamma=(\gamma_l-\gamma_r)/2$ are the total collision-induced broadening and the broadening difference in left and right QW's, respectively. Since the time scale of τ is of the order of $\hbar/\varepsilon_F$ and a typical t is of the order of $\hbar/\gamma_{eff}$ in the integrals of Eq. (24), we can replace $t^2-\tau^2/4$ by t^2, due to the quasiclassical condition $\gamma_{eff}\ll\varepsilon_F$, and the integration over τ gives us $2\pi\hbar\,\delta(\varepsilon_F-m(u/t)^2/2)$. After straightforward integration over $\mathbf{u}$ we finally obtain

$$\mathcal{G}(\Delta)\simeq\left(\frac{eT}{\hbar}\right)^2\rho_{2D}\int_{-\infty}^{0}dt\,e^{(\gamma+i\Delta)t/\hbar}\exp\left[-\frac{t^2}{2\hbar^2}W\left(\frac{v_Ft}{l_c}\right)\right]+\text{c.c.},\tag{25}$$

where $\rho_{2D}=m/\pi\hbar^2$ is the 2D density of states, the correla-

tion function is given by Eq. (23), and v_F is the Fermi velocity.

Consider first the limiting case of the local response, assuming

$$(v_F\hbar/\gamma_{eff}l_c)^2 \ll 1, \tag{26}$$

where the effective HWHM due to both contribution from collision processes and inhomogeneous broadening is determined by $\mathfrak{G}(\gamma_{eff})=\mathfrak{G}(0)/2$. Under such a condition the correlation function (23) assumes the form $W(u/l_c)\approx W(0)=\overline{\delta\varepsilon^2}$ and for conductance line shape from Eq. (25) it follows that[15]

$$\mathfrak{G}(\Delta)=2\left(\frac{eT}{\hbar}\right)^2\rho_{2D}\int_{-\infty}^{0}dt\,e^{\gamma t/\hbar-(\overline{\delta\varepsilon}t/\sqrt{2}\hbar)^2}\cos[(\Delta/\hbar)t]$$

$$=\frac{(eT)^2}{\hbar}\rho_{2D}$$

$$\times\begin{cases}2\gamma/(\Delta^2+\gamma^2), & \overline{\delta\varepsilon}\ll\gamma\\ (\sqrt{2\pi}/\overline{\delta\varepsilon})\exp[-(\Delta/\sqrt{2}\overline{\delta\varepsilon})^2], & \overline{\delta\varepsilon}\gg\gamma,\end{cases} \tag{27}$$

where the limiting cases determine the Lorentzian or Gaussian line shape. Notice that the Lorentzian shape of the peak tails is always found for big enough $|\Delta|$.

Now, consider the variables $t_{1,2}$ in the integral with the upper sign in Eq. (20). They are estimated of the order of $\hbar/\varepsilon_F$. Thus u is of the order of $\hbar/\sqrt{m\varepsilon_F}\ll l_c$, and as a result, we can replace the factor $\exp[-K_+(t_1,t_2,u)]$ by the expression $\exp[-(t_1-t_2)^2w(0)/(8\hbar^2)]$ where the exponential factor is of the order of $(\overline{\delta\varepsilon}/\varepsilon_F)^2\ll 1$ and the expression can be approximated by the unity. After straightforward integrations over $\mathbf{u}$ and τ, we are left with an integral over t given by

$$-i\frac{(eT)^2\rho_{2D}}{\pi\hbar^2}\int_{-\infty}^{0}dt\,e^{(\gamma_l+\gamma_r+i\Delta)t/\hbar}e^{-i2\varepsilon_F t/\hbar}+\text{c.c.}$$

$$\approx\frac{(eT)^2\rho_{2D}}{2\pi\hbar\varepsilon_F}. \tag{28}$$

Such a contribution can be discarded in comparison with the results from Eqs. (25) and (27) because this term leads to corrections of the order of $\gamma_{eff}/\varepsilon_F$.

In Fig. 2, we plot $\mathfrak{G}(\Delta)$, using Eq. (27), as function of Δ/γ for different relative contributions of the scattering processes and of the inhomogeneous broadening, i.e., for different ratios $\overline{\delta\varepsilon}/\gamma$. The solid, dashed, dotted, dot-dashed, and dot-dot-dashed curves in Fig. 2 correspond to $\overline{\delta\varepsilon}/\gamma=0.3$, 0.6, 1, 3, and 6, respectively. The factor $\mathfrak{G}_L(0)=2(eT)^2\rho_{2D}/\hbar\gamma$ is obtained by putting $\Delta=0$ and $\overline{\delta\varepsilon}=0$ in Eq. (27). We see in Fig. 2 that the change from a Lorentzian and a Gaussian line shapes depends also on the dimensionless ratio $|\Delta|/\gamma$.

If we take the opposite limit to the inequality (26), i.e., we are dealing now with relatively short l_c, then $W(v_Ft/l_c)$ in Eq. (25) has to be approximated by $W(x)/\overline{\delta\varepsilon^2}\approx\sqrt{\pi}x^{-1}$. As a result, the Lorentzian line shape is obtained, from Eq. (25), as

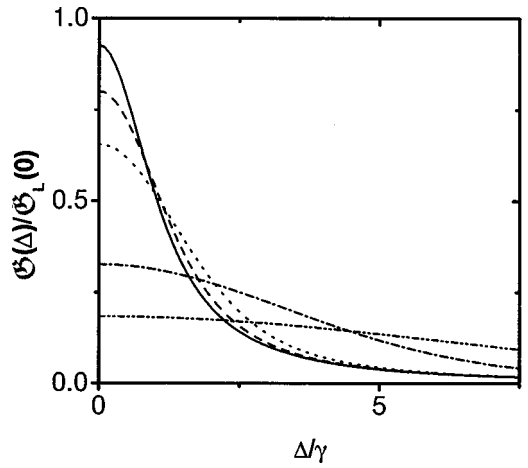

FIG. 2. Modified line shapes $\mathfrak{G}(\Delta)$, taken from Eq. (27), normalized by $\mathfrak{G}_L(0)=2(eT)^2\rho_{2D}/\hbar\gamma$, when nonlocal effects are negligible, for different contributions of short-range scattering, characterized by the phenomenological broadening parameter γ, and nonscreened large-scale disorder, characterized by $\overline{\delta\varepsilon}$ and l_c. The solid, dashed, dotted, dot-dashed, and dot-dot-dashed curves correspond to $\overline{\delta\varepsilon}/\gamma=0.3$, 0.6, 1, 3, and 6, respectively. The solid curve is almost a Lorentzian line shape, while the dot-dot-dashed curve is very close to a Gaussian curve.

$$\mathfrak{G}(\Delta)=\frac{(eT)^2}{\hbar}\rho_{2D}\frac{2\overline{\gamma}_{eff}}{\Delta^2+\overline{\gamma}_{eff}^2} \tag{29}$$

where the effective HWHM is now defined by $\overline{\gamma}_{eff}=\gamma[1+(\sqrt{\pi}/2)(\overline{\delta\varepsilon^2}l_c/\hbar v_F\gamma)]$. So, by increasing l_c, a transition from the Lorentzian to a Gaussian line shape is obtained for $\overline{\delta\varepsilon}>\gamma$.

This peak modification is illustrated in Fig. 3, where $\mathfrak{G}(\Delta)$, calculated from Eq. (25), is displayed for $\overline{\delta\varepsilon}/\gamma=4.6$. In Fig. 3, the solid, dashed, dotted, and dot-dashed curves correspond to $\hbar v_F/l_c\gamma=15$, 3.5, 0.7, and 0.2, respectively.

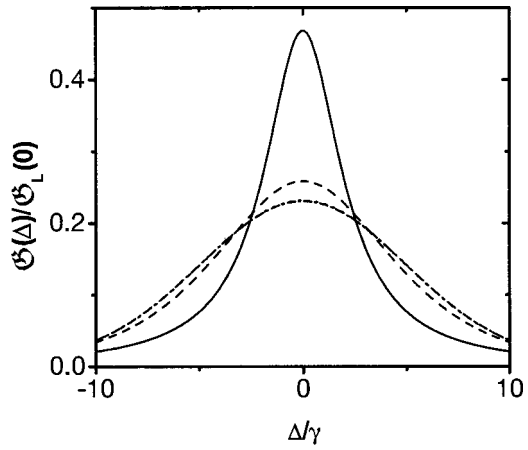

FIG. 3. Modified line shape $\mathfrak{G}(\Delta)$, calculated from Eq. (25), when nonlocal effects are taken into account, for $\overline{\delta\varepsilon}/\gamma=4.6$ and different values of $\hbar v_F/l_c\gamma$. The solid, dashed, dotted, and dot-dashed curves correspond to $\hbar v_F/l_c\gamma=15$, 3.5, 0.7, and 0.2, respectively and represents, for instance, the increase of l_c. Note that the line shape evolves practically from a Lorentzian (solid curve), given by Eq. (29), to a Gaussian one (dot-dashed curve).

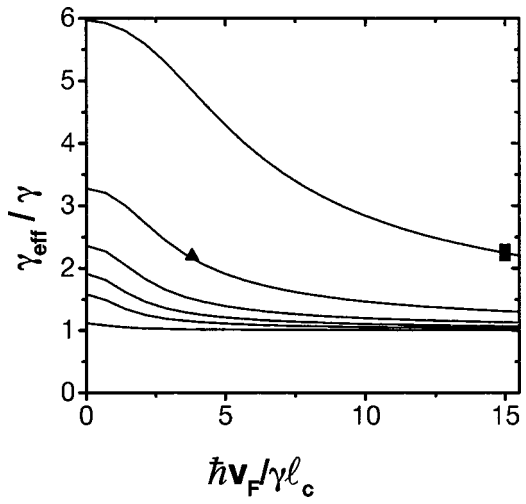

FIG. 4. Dimensionless tunnel resonance width γ_{eff}/γ as function of $\hbar v_F/l_c\gamma$, calculated from Eq. (25). The solid curves from top to bottom correspond to $\overline{\delta\varepsilon/\gamma}=4.6$, 2.3, 1.5, 1.1, 0.8, and 0.3. For $\hbar v_F/l_c\gamma=0$, nonlocal effects are negligible.

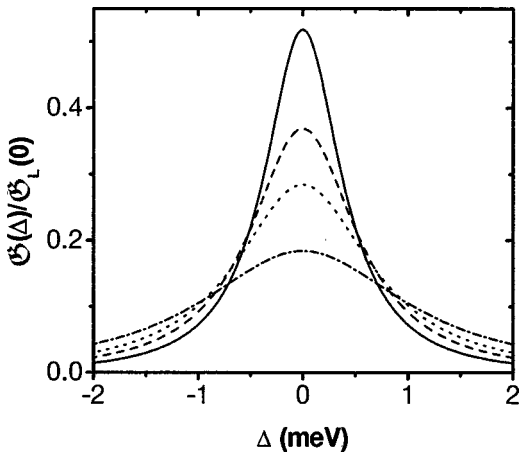

FIG. 5. Modified line shape $\mathfrak{G}(\Delta)$, for data of sample B of Ref. 5, calculated from Eq. (25), in which temperature effects were included. The solid, dashed, dotted, and dot-dashed curves correspond to temperatures 0.7, 5, 7, and 10 K, respectively. In $\mathfrak{G}_L(0)$ it was used $\gamma=0.2$ meV corresponding to the solid curve.

Notice that the solid curve corresponds very closely to the Lorentzian given by Eq. (29), while the dotted and the dot-dashed curves are practically coincident Gaussians. In Fig. 4, we plot γ_{eff}/γ, calculated from Eq. (25), as a function of $\hbar v_F/l_c\gamma$ for decreasing values of $\overline{\delta\varepsilon/\gamma}=4.6$ (top), 2.3, 1.5, 1.1, 0.8, and 0.3 (bottom). We point out that all curves give γ_{eff} in the local regime for $\hbar v_F/l_c\gamma=0$. Thus, from Fig. 4, it is seen that nonlocal effects essentially make γ_{eff} decrease for $\overline{\delta\varepsilon/\gamma}\gtrsim 1$.

Now we apply the present model calculation to interpret the experimental data of Ref. 5. First, we consider the results in the low-temperature regime (less than 2 K), where the measured HWHM γ_{eff} is practically independent of the temperature. We assume that only the inverted heterointerface for each QW has essential roughness[16] due to one-monolayer variations ($\overline{a}\approx 2.5$ Å) and, according to Appendix A, the characteristic energy is estimated as $\overline{\delta\varepsilon}\approx 0.46$ meV. The hard-wall model for a QW is used here to calculate $\overline{\varepsilon}$ from Eq. (A6). For sample A, with electron density 1.6×10^{11} cm^{-2}, we assume that $\gamma\approx 0.1$ meV (from mobility data) and $l_c\approx 700$ Å and obtain from the pertinent curve, for $\overline{\delta\varepsilon/\gamma}=4.6$, in Fig. 4, that $\gamma_{eff}\approx 0.22$ meV, which coincides with the experimental data and corresponds to $\hbar v_F/l_c\gamma=15$ (the solid square in Fig. 4). As a consequence, the Lorentzian line shape given by the solid curve in Fig. 3, is appropriate for sample A. Furthermore, for sample B, with density 1.5×10^{11} cm^{-2}, by assuming that $\gamma\approx 0.2$ meV and $l_c\approx 1400$ Å, we obtain $\gamma_{eff}\approx 0.45$ meV from the pertinent curve, for $\overline{\delta\varepsilon/\gamma}=2.3$, in Fig. 4, after using the calculated value $\hbar v_F/l_c\gamma=3.8$ (the solid triangle). This value is in good agreement with the experimental result of Ref. 5. For sample C, with density 0.8×10^{11} cm^{-2} and assuming $\gamma\approx 0.2$ meV and $l_c\approx 1000$ Å, we have $\gamma_{eff}\approx 0.45$ meV (indicated by the solid triangle in Fig. 4), i.e., the same as for sample B and also coincident with experimental observations.[5] Then a good agreement with the experimental results is found for the case of single-side variations of heterointerfaces (see Ref. 17 about the case of two-side variations).

Notice that the change from a local regime of tunneling (for long-range fluctuations of QW widths) to the general nonlocal case may be found by varying the temperature that controls the relative contributions of homogeneous and inhomogeneous broadening. In Fig. 5 we plot the line shapes $\mathfrak{G}(\Delta)$, for temperatures Θ in the range 0.7 K–10 K, calculated from Eq. (25), for sample B parameters taken from Ref. 5. Now we have to add the thermal e-e scattering contribution to γ, leading to a renormalized value $\gamma(\Theta)$, which we approximate in the same way as in Ref. 5 (see the solid curve in Fig. 3 of Ref. 5). In Fig. 5, the solid, dashed, dotted and dot-dashed curves correspond to $\Theta=0.7$, 5, 7, and 10 K, respectively. One can see that by decreasing the temperature, the linewidth becomes smaller and the shape of peak is changed. While for $\Theta=0.7$ K, we observe a Lorentzian form of the peak due to strong nonlocal effects, manifested by inhomogeneous broadening induced by nonscreened large-scale fluctuations, nonlocal effects are quite weak for $\Theta=10$ K. At this temperature the local regime prevails and the line shape is the interplay of Gaussian and Lorentzian forms, given by Eq. (27), because in this case $\overline{\delta\varepsilon/\gamma(\Theta)}\approx 0.5$ and $\hbar v_F/l_c\gamma(\Theta)\approx 0.8$ the peak behavior is slightly more Lorentzian than Gaussian.

IV. CONCLUDING REMARKS

In the present work, we have introduced an alternative electron scattering mechanism by long-scale nonscreened roughness of heterointerfaces that contributes to the inhomogeneous broadening of the tunneling conductance peak in coupled DQW's. We have done a systematic analysis of this peak shape by taking into account the interplay between the introduced mechanism and the usual homogeneous scattering broadening. A detailed comparison of the HWHM of the peak with experimental results revealed that the considered mechanism is relevant to interpret the data of Ref. 5, because in the experimental conditions strong nonlocal effects are

manifested, through the proposed mechanism of inhomogeneous broadening, which modify drastically the line shape (from the Gaussian to a Lorentzian) and the HWHM of the peaks. We call attention to general considerations for the mechanism of appearance of nonscreened long-wavelength variations of the scattering potential, given in Appendix A, which should be relevant not only for the problem of inter-QW tunneling current, addressed here, but also for the study of general transport and optical properties of doped DQW's.

Let us discuss the approximations used in our treatment. The single-electron approximation for the tunneling Hamiltonian in Sec. II is a generally accepted model and the expression for the tunneling current in the homogeneous case corresponds to the Bardeen's approach.[18] Here smooth variations of boundaries lead to changes of the levels of left and right QW's in the tunneling Hamiltonian, and we assume that small modifications of the tunneling matrix element can be neglected. For a discussion of the latter approximation, see Ref. 10. The approximation for considering the screening ''on average'' in the introduced large-scale potential involves supposing that the correlation length l_c is large in comparison with the Bohr radius and with transverse dimensions of the DQW structure as well. Since $\mathfrak{G}(\Delta)$ depends on the sum of the scattering broadening of different levels, we believe that the introduction of phenomenological parameters $\gamma_{l,r}$ instead of a detailed consideration the self-energy functions, does not lead to the omission of important contributions. We have also used the quasiclassical description for longitudinal motion that is valid when $\varepsilon_F \gg \gamma_{eff}$ in the calculation of the path integrals in Eq. (18) and for integration over $\mathbf{u}$ and τ in Eq. (24). We have assumed that variations of potential are sufficiently weak such that the acceleration of an electron due to a long-scale random force (quasielectric field) on a length of the order of l_c is insignificant. We have considered that the inverted $Al_xGa_{1-x}As$-GaAs heterointerface is much more rougher than the normal GaAs-$Al_xGa_{1-x}As$ heterointerface based on the results of Ref. 16 for QW's similar to those used in DQW structures of Ref. 5.

To conclude, we now discuss the possibility of a more reliable test of the described mechanism of inhomogeneous broadening. In further experimental studies of the tunneling conductance it is necessary to make a more detailed analysis of the line-shape transition (from the Lorentzian to Gaussian form), and comparison between HWHM data measured in samples grown in different conditions. Because the considered mechanism modifies also in-plane transport coefficients and optical properties of DQW's with long-wavelength inhomogeneities, further measurements as well theoretical studies of these phenomena are necessary.

We believe that the present work establishes an essential contribution of large-scale nonscreened fluctuations to the broadening of the tunneling conductance peak in DQW's in agreement with experimental results.[5]

ACKNOWLEDGMENTS

This work was supported by Grants Nos. 95/0789-3 and 98/10192-2 from Fundação de Amparo à Pesquisa de São Paulo (FAPESP). O.G.B. and N.S. are grateful to Conselho Nacional de Desenvolvimento Científico e Tecnológico (CNPq) for financial support.

APPENDIX A: NONSCREENED VARIATIONS OF THE RANDOM POTENTIAL

Below we evaluate the nonscreened random contributions to the potential $\pm\delta U_{\mathbf{x}}$ that appears in Eqs. (2)–(4). The 2D Fourier transform of the screening potential, $V_{\mathbf{qz}}$, is determined by the Poisson equation

$$\left(\frac{d^2}{dz^2}-q^2\right)V_{\mathbf{qz}}=-\frac{4\pi e^2}{\epsilon}\delta n_{\mathbf{qz}}, \tag{A1}$$

where $\delta n_{\mathbf{qz}}$ is the concentration induced by the total large-scale potential. Neglecting the overlap of left and right orbitals φ_{jz} $(j=l,r)$ we use in Eq. (A1) the expansion

$$\delta n_{\mathbf{qz}}=\sum_{j=l,r}\delta n_{\mathbf{q}j}\varphi_{jz}^2, \tag{A2}$$

where $\delta n_{\mathbf{q}j}=-\rho_{2D}(\overline{U}_{\mathbf{q}j}+V_{\mathbf{q}j})$ is the in-plane induced concentration in the jth QW due to slow variations of the potential while the nondiagonal components of $\delta\hat{n}_{\mathbf{x}}$ are small due to weak overlap of left and right orbitals. Note that, for the general case of slowly varying heterointerfaces, $\varphi_{j\mathbf{x}z}$ should depend on the in-plane coordinate $\mathbf{x}$ but for the 2D case $(\varepsilon_F \ll \varepsilon_j)$ such in-plane variations of orbitals are not important.

The solution of Eq. (A1) assumes the form

$$V_{\mathbf{qz}}=\frac{2\pi e^2}{\epsilon q}\int dz' e^{-q|z-z'|}\delta n_{\mathbf{q}z'}, \tag{A3}$$

where for the case $q\lesssim l_c^{-1}\ll d^{-1}$ we have $\exp(-q|z-z'|)\simeq 1$. Then the diagonal components $V_{\mathbf{q}j}$, $j=l,r$, are expressed in terms of the total concentration as

$$V_{\mathbf{q}j}=\int dz\varphi_{jz}^2 V_{\mathbf{qz}}=\frac{2\pi e^2}{\epsilon q}\sum_{s=l,r}\delta n_{\mathbf{q}s}. \tag{A4}$$

Substituting $\delta n_{\mathbf{q}j}$ in Eq. (A4), we have

$$V_{\mathbf{q}j}=-\frac{2}{qa_B}\sum_{s=l,r}(\overline{U}_{\mathbf{q}s}+V_{\mathbf{q}s}), \tag{A5}$$

where a_B is the Bohr radius. Since the right-hand side of Eq. (A5) does not depend on j we obtain $V_{\mathbf{q}l,r}=V_{\mathbf{q}}$ and we deal with an averaged screened potential $V_{\mathbf{q}}$ across the DQW's. If we assume large-scale variations, and a thin DQW, we derive Eq. (2), $V_{\mathbf{q}}\simeq-(\Sigma_j\overline{U}_{\mathbf{q}j})/2$.

Now we present explicit expressions for the large-scale addends to the matrix Hamiltonian (1) due to the random variations of the DQW heterointerfaces. Statistically independent boundaries variations are described by random functions $\delta_{\mathbf{x}}^{<}$ and $\delta_{\mathbf{x}}^{>}$ [see Fig. 1(b)] so that large-scale potentials take the form $\overline{U}_{l,r\mathbf{x}}\simeq 2\varepsilon_{l,r}(\delta_{\mathbf{x}}^{<}-\delta_{\mathbf{x}}^{>})/d_{l,r}$, where $\varepsilon_{l,r}$ are the energies of levels in left and right QW's with width $d_{l,r}$. As it was shown in Ref. 8, the weak contributions due to variations of the tunneling matrix element may be neglected in the evaluation of Eq. (8) up to second-order in T. Substituting

$\overline{U}_{l,r\mathbf{x}}$ into the correlation functions in Eq. (4) and supposing that all interfaces are statistically equivalents, we obtain the correlation functions as

$$\overline{W}_{l,r}(|\mathbf{x}-\mathbf{x}'|)=2\left(\frac{2\overline{\varepsilon a}}{\overline{d}}\right)^2\exp\left[-\left(\frac{\mathbf{x}-\mathbf{x}'}{l_c}\right)^2\right], \qquad \text{(A6)}$$

where $\overline{\varepsilon}\simeq\varepsilon_{l,r}$, $\overline{d}\simeq d_{l,r}$, $\overline{a}$ is the averaged deviation of heterointerfaces and l_c is the correlation length. Finally, the correlation function $w(|\cdots|)$ in Eq. (4) takes the form $w(|\mathbf{x}-\mathbf{x}'|)=(\overline{\delta\varepsilon})^2\exp[-(\mathbf{x}-\mathbf{x}')^2/l_c^2]$ with a characteristic energy $\overline{\delta\varepsilon}=4\overline{\varepsilon a}/\overline{d}$ for the case of two-side variations. However, $\overline{\delta\varepsilon}=2\sqrt{2}\overline{\varepsilon a}/\overline{d}$ for the one-side variation case in a QW when $\delta_{\mathbf{x}}^{<}$ or $\delta_{\mathbf{x}}^{>}$ is equal to zero and one of the two correlation functions given by Eq. (A6) is set to zero.

APPENDIX B: OPTIMAL FLUCTUATION METHOD

The evaluation of the Eq. (20) is based on the separation of the optimal trajectory (with maximal contribution to the path integral) and on the comparison of typical variations to such a trajectory, $\delta\mathbf{x}_\tau$ and $\delta\mathbf{y}_\tau$, with l_c. First variations of the actions in the exponential factors of Eqs. (18) and (19) with respect to path variations $\delta\mathbf{x}_\tau$ and $\delta\mathbf{y}_\tau$ are written as follows:

$$-\frac{i}{\hbar}\int_0^{t_1}d\tau\,\delta\mathbf{x}_\tau\cdot\left\{m\ddot{\mathbf{x}}_\tau-\frac{i}{2\hbar l_c^2}\int_0^{t_1}d\tau'[\mathbf{u}(\tau-\tau')/t_1+\mathbf{x}_\tau-\mathbf{x}_{\tau'}]w(|\mathbf{u}(\tau-\tau')/t_1+\mathbf{x}_\tau-\mathbf{x}_{\tau'}|)\pm\frac{i}{2\hbar l_c^2}\int_0^{t_1}d\tau'\left[\mathbf{u}\left(\frac{\tau}{t_1}-\frac{\tau'}{t_2}\right)\right.\right.$$
$$\left.\left.+\mathbf{x}_\tau-\mathbf{y}_{\tau'}-\frac{\mathbf{u}}{2}(1\pm1)\right]w\left(\left|\mathbf{u}\tau/t_1+\mathbf{x}_\tau-\mathbf{u}\tau'/t_2-\mathbf{y}_{\tau'}-\frac{\mathbf{u}}{2}(1\pm1)\right|\right)\right\}, \qquad \text{(B1)}$$

and

$$-\frac{i}{\hbar}\int_0^{t_2}d\tau\delta\mathbf{y}_\tau\cdot\left\{\pm m\ddot{\mathbf{y}}_\tau-\frac{i}{2\hbar l_c^2}\int_0^{t_2}d\tau'[\pm\mathbf{u}(\tau-\tau')/t_2+\mathbf{y}_\tau-\mathbf{y}_{\tau'}]w(|\pm\mathbf{u}(\tau-\tau')/t_2+\mathbf{y}_\tau-\mathbf{y}_{\tau'}|)\pm\frac{i}{2\hbar l_c^2}\right.$$
$$\left.\times\int_0^{t_1}d\tau'\left[\mathbf{u}\left(\frac{\tau}{t_2}-\frac{\tau'}{t_1}\right)-\mathbf{x}_{\tau'}+\mathbf{y}_\tau-\frac{\mathbf{u}}{2}(1\pm1)\right]w\left(\left|\mathbf{u}\tau'/t_1+\mathbf{x}_{\tau'}-\mathbf{u}\tau/t_2-\mathbf{y}_\tau+\frac{\mathbf{u}}{2}(1\pm1)\right|\right)\right\}, \qquad \text{(B2)}$$

where the upper (lower) signs correspond to upper (lower) signs in Eqs. (18) and (19) and we have transformed correlation functions as follows:

$$w(|\mathbf{x}+\delta\mathbf{x}|)-w(|\mathbf{x}|)\simeq-2\mathbf{x}\cdot\delta\mathbf{x}w(x)/l_c^2. \qquad \text{(B3)}$$

Since $\delta\mathbf{x}_\tau$ and $\delta\mathbf{y}_\tau$ are arbitrary variations, the optimal trajectories are determined by the system of Euler-Lagrange equations as

$$m\ddot{\mathbf{x}}_\tau=\frac{i}{2\hbar l_c^2}\int_0^{t_1}d\tau'[\mathbf{u}(\tau-\tau')/t_1+\mathbf{x}_\tau-\mathbf{x}_{\tau'}]$$
$$\times w(|\mathbf{u}(\tau-\tau')/t_1+\mathbf{x}_\tau-\mathbf{x}_{\tau'}|)\mp\frac{i}{2\hbar l_c^2}$$
$$\times\int_0^{t_2}d\tau'[\mathbf{u}(\tau/t_1-\tau'/t_2)+\mathbf{x}_\tau-\mathbf{y}_{\tau'}-\mathbf{u}(1\pm1)/2]$$
$$\times w(|\mathbf{u}\tau/t_1+\mathbf{x}_\tau-\mathbf{u}\tau'/t_2-\mathbf{y}_{\tau'}-\mathbf{u}(1\pm1)/2|), \qquad \text{(B4)}$$

and

$$\pm m\ddot{\mathbf{y}}_\tau=\frac{i}{2\hbar l_c^2}\int_0^{t_2}d\tau'[\pm\mathbf{u}(\tau-\tau')/t_2+\mathbf{y}_\tau-\mathbf{y}_{\tau'}]$$
$$\times w(|\pm\mathbf{u}(\tau-\tau')/t_2+\mathbf{y}_\tau-\mathbf{y}_{\tau'}|)\mp\frac{i}{2\hbar l_c^2}$$
$$\times\int_0^{t_1}d\tau'[\mathbf{u}(\tau/t_2-\tau'/t_1)-\mathbf{x}_{\tau'}+\mathbf{y}_\tau-\mathbf{u}(1\pm1)/2]$$
$$\times w(|\mathbf{u}\tau/t_2+\mathbf{y}_\tau-\mathbf{u}\tau'/t_1-\mathbf{x}_{\tau'}-\mathbf{u}(1\pm1)/2|). \qquad \text{(B5)}$$

In order to estimate the maximal deviations, $x_{\max}$ and $y_{\max}$, we suppose that $u\tau_{1,2}^{\max}/t_{1,2}\gg|x_{\max}|,|y_{\max}|$ for typical parameters used in calculating $\mathfrak{G}(\Delta)$ such that $x_{\max}=x_{\tau_1^{\max}}$ and $y_{\max}=y_{\tau_2^{\max}}$. Thus, the right-hand sides of Eqs. (B4) and (B5) do not depend on $\mathbf{x}_\tau$ and $\mathbf{y}_\tau$ and they can be easily integrated with the boundary conditions $\mathbf{x}_{\tau=0,t_1}=\mathbf{0}$ and $\mathbf{y}_{\tau=0,t_2}=\mathbf{0}$. For the upper-sign contributions, estimating $\mathbf{u}w(|\mathbf{u}|)|\approx l_c\overline{\delta\varepsilon^2}$ we transform the right-hand sides of Eqs. (B4) and (B5) into $i\overline{\delta\varepsilon^2}(|t_1|+|t_2|)/(2m\hbar l_c)$. Thus, the result for the maximal deviations is

$$\left|\begin{matrix}x_{\max}\\ y_{\max}\end{matrix}\right|\simeq\frac{\overline{\delta\varepsilon^2}(|t_1|+|t_2|)}{16m\hbar l_c}\left|\begin{matrix}t_1^2\\ t_2^2\end{matrix}\right|. \qquad \text{(B6)}$$

This satisfies the condition $|x_{\max}|,|y_{\max}|\ll l_c$ for the upper-sign contributions because $t_{1,2}$ are estimated as $\hbar/\varepsilon_F$. Indeed,

then we have $|x_{\max}|/l_c$ and $|y_{\max}|/l_c \approx (\overline{\delta\varepsilon/\varepsilon_F})^2(\varepsilon_c/4\varepsilon_F) \ll 1$, where the characteristic energy $\varepsilon_c = (\hbar/l_c)^2/2m \ll \varepsilon_F$.

A more careful consideration is necessary for the lower-sign contributions when $|t_1 - t_2| \lesssim \hbar/\varepsilon_F$, such that $t_{1,2} \approx t$. Thus, Eq. (B4) can be rewritten as

$$\ddot{\mathbf{x}}_\tau \approx \frac{i\mathbf{u}\overline{\delta\varepsilon^{\,2}}t}{m\hbar l_c^2}\int_0^1 dz'(z-z')\exp[-u^2(z'-z)^2/l_c^2], \tag{B7}$$

where $z = \tau/t$. Here, from Eq. (B5), it follows that $\ddot{\mathbf{y}}_\tau \approx 0$, and taking into account the boundary conditions, $\mathbf{y}_{\tau=0,t_2} = \mathbf{0}$, we are led to $\mathbf{y}_\tau \approx \mathbf{0}$. It is easy to solve Eq. (B7) taking into account in its right-hand side that for the lower-sign contributions $t \gg \tau$, as it was shown in Sec. IV, due to the fact that $\varepsilon_F \gg \gamma_{eff}$. Then solving Eq. (B7), with boundary conditions $\mathbf{x}_{\tau=0,t_1} = \mathbf{0}$, we obtain the maximal deviation $|x_{\max}|$ as

$$|x_{\max}| \approx \frac{\overline{\delta\varepsilon^{\,2}}t^3}{16m\hbar l_c}F_x(u/l_c), \tag{B8}$$

where $F_x(z) = [1-\exp(-z^2)]/z$ and $F_x(z) \approx z$, for $z^2 \ll 1$, while $F_x(z) \approx 1/z$, for $z^2 \gg 1$ and the maximum of $F_x(z) < 0.65$ corresponds to z close to the unity. This estimation practically coincides with Eq. (B6) if $u/l_c \sim 1$, while the maximal deviations are smaller than the results in Eq. (B6) both for $u/l_c \ll 1$ and $u/l_c \gg 1$.

*On leave from Institute of Semiconductor Physics, Kiev, National Academy of Sciences of Ukraine, 252650, Ukraine.

[1] R. Tsu and L. Esaki, Appl. Phys. Lett. **22**, 562 (1973).
[2] P. Mazumder, A. Kulkarni, M. Bhattacharya, J. P. Sun, and G. I. Haddad, Proc. IEEE **86**, 664 (1998).
[3] J. Smoliner, W. Demmerle, G. Berthold, E. Gornik, G. Weimann, and W. Schlapp, Phys. Rev. Lett. **63**, 2116 (1989).
[4] J. P. Eisenstein, L. N. Pfeiffer, and K. W. West, Appl. Phys. Lett. **57**, 2324 (1990).
[5] S. Q. Murphy, J. P. Eisenstein, L. N. Pfeiffer, and K. W. West, Phys. Rev. B **52**, 14 825 (1995).
[6] J. A. Simmons, M. A. Blount, J. S. Moon, S. K. Lyo, W. E. Baca, J. R. Wendt, J. L. Reno, and M. J. Hafich, J. Appl. Phys. **84**, 5626 (1998).
[7] F. T. Vasko, J. P. Sun, G. I. Haddad, and V. V. Mitin, J. Appl. Phys. **87**, 3582 (2000).
[8] O. G. Balev, F. T. Vasko, F. Aristone, and N. Studart, Phys. Rev. B (to be published).
[9] M. Fogler, A. A. Koulakov, and B. I. Shklovskii, Phys. Rev. B **54**, 1853 (1996).
[10] F. T. Vasko and O. E. Raichev, Phys. Rev. B **50**, 12 195 (1994); Zh. Éksp. Teor. Fiz. **107**, 951 (1995) [JETP **80**, 539 (1995)].
[11] L. Zheng and A. H. MacDonald, Phys. Rev. B **47**, 10 619 (1993).
[12] O. E. Raichev and F. T. Vasko, J. Phys.: Condens. Matter **8**, 1041 (1996); **9**, 1547 (1997).
[13] L. S. Schulman, *Techniques and Applications of Path Integration* (Wiley, New York, 1981).
[14] B. I. Halperin and M. Lax, Phys. Rev. **148**, 722 (1966).
[15] Notice that the general form of Eq. (27) may be obtained by averaging the Lorentz peak with a random level splitting $\Delta_{\mathbf{x}}$. The essential point here is the condition of the local regime, given by Eq. (26).
[16] L. N. Pfeiffer, E. F. Schubert, and K. W. West, Appl. Phys. Lett. **58**, 2258 (1991).
[17] For two-side variations of heterointerfaces, as in Eq. (A6), we obtain $l_c = 350$ Å, 700 Å, and 500 Å for samples A, B, and C, respectively. Because in Ref. 5 it is reported that 200 Å QW's are separated by the tunnel barriers with 175 Å to 350 Å (even though the real values are not given samples for A, B, and C) and considering the results of Ref. 16, we have assumed here only one-side fluctuations of the QW for samples in Ref. 5.
[18] J. Bardeen, Phys. Rev. Lett. **6**, 57 (1961).